

# GOLDEN RATIO ENTROPIC GRAVITY: GRAVITATIONAL SINGULARITY “FIELD” TESTING

30<sup>th</sup> April 2019.

Stephen H. Jarvis.

<http://orcid.org/0000-0003-3869-7694> (ORCID)

EQUUS AEROSPACE PTY LTD

Web: [www.equusspace.com](http://www.equusspace.com)

email: [shj@equusspace.com](mailto:shj@equusspace.com)

**Abstract:** In taking up from the preliminary papers [1][2][3][4][5][6] regarding the golden ratio algorithm for time, specifically paper 5 [5] regarding entropy and enthalpy, and paper 6 [6] regarding the golden ratio algorithm for the idea of the relativity of time, the key focus of this paper is the process of gravity emerging from electrodynamics and how that can be demonstrated per experiment. First, the nature of gravity as an emergent feature as per the golden ratio time-algorithm is discussed, highlighting mathematically its nature in space as a “singularity” that allows for the idea of kinetic energy, a feature known to co-exist with the idea of gravity. Two key experiments for gravity emerging from electrodynamics are then proposed, tested, the results of which then discussed, shedding new and important light on current “RF Resonant Cavity Thruster (EM-drive)” research.

**Keywords:** time; space; golden ratio; theta; gravity; quantum gravity; electromagnetism; emergent gravity; Fibonacci sequence; wave-function; relativity; entropy; enthalpy; Dirac; Dirac sea; antiparticle; positron; anti-matter; fractal; conservation of energy; conservation of momentum; EM-drive; cavity thruster; microwave; RF; warp drive; resonant cavity; gravielectric

---

## 1. INTRODUCTION

Science is essentially "two paradigms"; the first is data, the second is theory as data explaining data. Understandably science moves forward with data and associated theory supporting that data, theory that can point

to if not predict new data (which is essentially a gold standard for a theory's success). The Achilles heel of science though is holding on to theories that could be explained much more simply; not data, yet "theories" that made data relating with data inefficient by being too complicated and tangled. As we develop as a species, data explaining data ideally becomes a more "efficient" construct, as demonstrated with our development of technology. The same should also be true with theory, data explaining data. The greatest problem science faces is learning how to make that "more efficient step" for data explaining data, casting away inefficient theories, in favour of new more "efficient" theories, of data explaining data, new theories that can predict new phenomena that old inefficient theories cannot.

The common theme throughout the preceding 6 papers has been presenting a case for a new "algorithm" for time; this algorithm for time was introduced and outlined in paper 1 [1], providing utility to the equations for gravity and electromagnetism (which were then followed up in paper 4 [4]). The question in presenting a paper that re-defines time (and thus a paper that must then must account for all the concepts of physics theory) is "where to start and how to develop that explanation, and in what priority of ideas?". So, in paper 1 [1], in being as basic as possible, the equations for gravity and electromagnetism were introduced, together with the Rydberg equation (electron shell modelling), to account for how time would dynamically exist in an atomic structure. Paper 2 [2] then presented a wave-function to account for this dynamic. Paper 3 [3] then presented the ideas of Brownian motion, a cornerstone idea for Einstein's preliminary work. Paper 4 [4] presented a closer look at the elementary particle dynamics regarding the newly proposed wave-function, and how this scales-up in a virtual Fibonacci-style extra-atomic manner, presenting the idea of Avogadro's number. Paper 5 [5] then presented the idea of time as "energy", and how this relates to the CMB radiation through the virtual Fibonacci-style stepping up process of a basic atomic structure as a process of time, linking key observed measurements together, providing a glimpse to the overall energy manifold dynamic of time and space as entropy and enthalpy. Finally, paper 6 [6] addressed the idea of the "relativity" of time, expanding upon the energy dynamic of the cosmos, coupling in the idea of the red-shift and CMB radiation, and the "end-zone" region of time-space to give an account of the most logical "image" of reality from within that overall time-space manifold using this new definition for time. Ideas of time and distance were then married up with known observed values of the universe.

The previous 6 key papers [1][2][3][4][5][6] introduced a theory for the golden ratio as time as a more efficient way of tackling the idea of a quantum wave-function, replacing complicated mathematical inertial transformation matrices. Further to this, the idea of relativity was explained more efficiently using the idea of the relativity of time, not space, yet "time" being the definitive a-priori in the analysis of relativity. The previous 6 key papers though have still failed to address the fundamental nature of gravity as an emergent feature of the atom as per the nature of a fundamental golden ratio variable, and in this case gravity as the  $(-\frac{1}{\varphi})^2$  feature of electromagnetism, and how this relates to the behaviour of electromagnetism on the emergent level. Here in this paper, the previous work on this subject of time as the golden ratio shall be given a final refurbishment outlining the precise link between the emergent features of electromagnetism and gravity as  $\varphi$  and  $(-\frac{1}{\varphi})^2$  respectively.

## 2. "NEGATIVE ENERGY" V "EMERGENT GRAVITY"

The general  $\varphi$  and  $(-\frac{1}{\varphi})^2$  entropic manifolds of emergent electromagnetic and gravitational energy respectively were outlined in paper 5 [5], with greater emphasis there in that paper on emergent electromagnetism and its relationship to the CMBR. Now we need to explain the other emergent feature of the atom, namely gravity, which as the entropic realm ([5]; p 8-9), as  $(-\frac{1}{\varphi})^2$ , would be a form of energy release. As per paper 5 [5], the formation of the phi-quantum wave-function for the atom on the elementary particle level is more or less enthalpic as it

undergoes a “contractive” dynamic process; see ([2]; eq.8, p12), ([2]; fig.16, p16), and ([4]; p3-4). Beyond this is emergent entropic electromagnetic radiation. Similarly, the formation of matter itself on the elementary particle level would be “enthalpic”, yet its emergence as “gravity” would be considered to be “entropic”.

The contemporary explanation for “entropic” gravity as kinetic energy associated to gravitational energy is simple: as the strength of the gravitational attraction between two objects represents the amount of gravitational energy [7] in the field which attracts them towards each other, when two objects are infinitely far apart the gravitational attraction and hence energy is close to zero. Yet when the two objects move towards each other, their motion accelerates by their mutual effect of gravity which causes an increase in the positive kinetic energy of the system. Yet, at the same time, the gravitational attraction (and thus energy) also increases in magnitude. The problem here is that the law of energy conservation [8] requires that the net energy of the system cannot change. Therefore, the change in gravitational energy must be negative to cancel out the positive change in kinetic energy. Paradoxically though, as the gravitational energy is *getting stronger*, this decrease can only mean that it is negative. There are a few problems with this idea though in the absence of negative energy, namely that in a universe in which positive energy dominates everything will eventually collapse in a “big crunch”, while in an “endless” universe where negative energy dominates everything will either expand indefinitely or cause a “big rip”. In a zero-energy universe [9] model (“flat” or “Euclidean”, the model proposed here), the total amount of energy in the universe is exactly zero where the amount of positive energy in the form of matter is exactly cancelled out by its negative energy in the form of gravity.

When the idea of negative energy is discussed, the idea of anti-particles cannot be ignored, as it is embedded in the current idea of negative energy; in regard to anti-particles, more specifically the positron, Dirac associated his “Dirac sea” as full of negative energy with “anti-particles” as a theoretical model of the vacuum containing an infinite sea of particles with negative energy [10]. Negative energy was first postulated to explain the anomalous negative-energy quantum states predicted by the Dirac equation [11] for relativistic electrons. The positron [12], the antimatter [13] counterpart of the electron, was originally conceived of as a hole in the Dirac sea, well before its experimental discovery in 1932. This idea was revised; although quantum field theory replaced the idea of the Dirac sea owing to the notion of anti-particles representing “real” matter, the theory presented a new explanation for anti-matter in paper 4 ([4]; p8-10), the idea of the positron being as an electron that has undergone a magnetic field “flip”, the case in point regarding the relationship here between positron and electron as a new explanation for a relativistic electron that when becoming super-massive would undergo a magnetic flip according to the phi-quantum wave-function. The question though with this theory, as per the phi-quantum wave-function, is why would there be a magnetic flip in the electron? The thinking is that electron in reaching relativistic speeds would undergo a magnetic flip according to the phi-quantum wave-function where the wavefunction would track back on itself as though mirroring the magnetic moment of the proton in taking on the signature of a massive particle at such a relativistic speed. It's not a remarkable concept in this phi-quantum wave-function golden ratio theory, just a derivative of a newly-defined process for time as the golden-ratio, yet a theoretical and research-based explanation. Therefore, the “idea” of anti-particles will not be used here in the process of describing “negative energy gravity”. The idea used here in this paper is “entropic” emergent gravity, which by its very nature in being entropic allows for this increase in kinetic energy of its associated mass (being enthalpic); to properly explain this process, a further step of equations and field modelling for time is required.

### 3. GRAVITATIONAL SINGULARITY FIELD MODELLING

The idea of gravity emerging as a  $(-\frac{1}{\phi})^2$  entity, a squaring of the phi-quantum wave-function idea, would on an emergent level present as an EM wave-function that in all appearance would be electromagnetically “silent”, as it

is essentially an electromagnetic wave that has undergone destructive interference as a standing wave, a resonance on itself. Previous papers described the process as for example paper 4 ([4]; fig.2, p.5), here as figure.1.

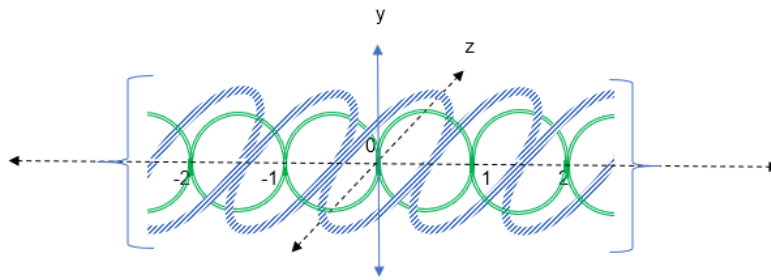


**Figure 1:** Green line electrical component (x-y), blue line magnetic component (x-z), both waves out of phase with each other and perpendicular to each other, folded-over/coupled. The values on the x-axis represent 1/2 quantum length increments.

This serves as an example of the idea of an EM folded field orientation. Beyond just considering the folded EM field, this quantum-gravity wave-function construct (folded EM field) would be associated to mass, or more precisely, would be a “carrier” of the mass-effect of “gravity”, the elementary particle pre-cursor of gravity. What are we looking for though regarding the emergence of gravity? To answer that question, we need to consider an all-together new paradigm that associates gravity with electromagnetism in the context of the golden ratio algorithm for time.

### 3.1 TIME EQUATIONS

- |  |     |   |
|--|-----|---|
| $t_B + 1 = t_B^2, t_B + 1 = t_A, t_B^2 = t_A$                | (1) | STANDARD GOLDEN RATIO TIME-EQUATIONS  |
| $\varphi + 1 = \varphi^2$                                    | (2) | EM ( $t_B$ )  |
| $\frac{-1}{\varphi} + 1 = \left(\frac{-1}{\varphi}\right)^2$ | (3) | GRAVITY ( $t_A$ )   |
| $\varphi \cdot \frac{-1}{\varphi} + 1 = 0$                   | (4) | TIME-SPACE ( $t_B$ as $\varphi \cdot \frac{-1}{\varphi}$ ) EQUATION   |
|  | -   | $t_B^2$ as gravity becomes as a “0”, as though it is natural to “0” space, and yet as a concept of time $t_A$ is as 0, as though immediate in 0-space.  |
| $\varphi \cdot \frac{-1}{\varphi} + (1 + 1) = 1$             | (5) | TIME EQUATION AMENDED AS SINGULARITY FIX  |
|  | -   | To <b>fix</b> gravity and thus make $t_A$ “1” ( $t_B^2 = t_A$ ) a “now” fix is needed, which as time represents “energy” [5], and thus energy is manifested with gravity as a “1” <b>singularity</b> , an extra $t_N$ . |

Equations 4 and 5 need proper explanation. Figure 2 aims to do this by considering a different approach to the equations for time using the golden ratio, a symbolic field/plane representation for time as a singularity (value of “1”) which then lends to the idea of a gravitational singularity as a field-effect as it extends to an event horizon value of “0” as  $t_A$ .

**GOLDEN RATIO TIME "FIELD" MODELLING**

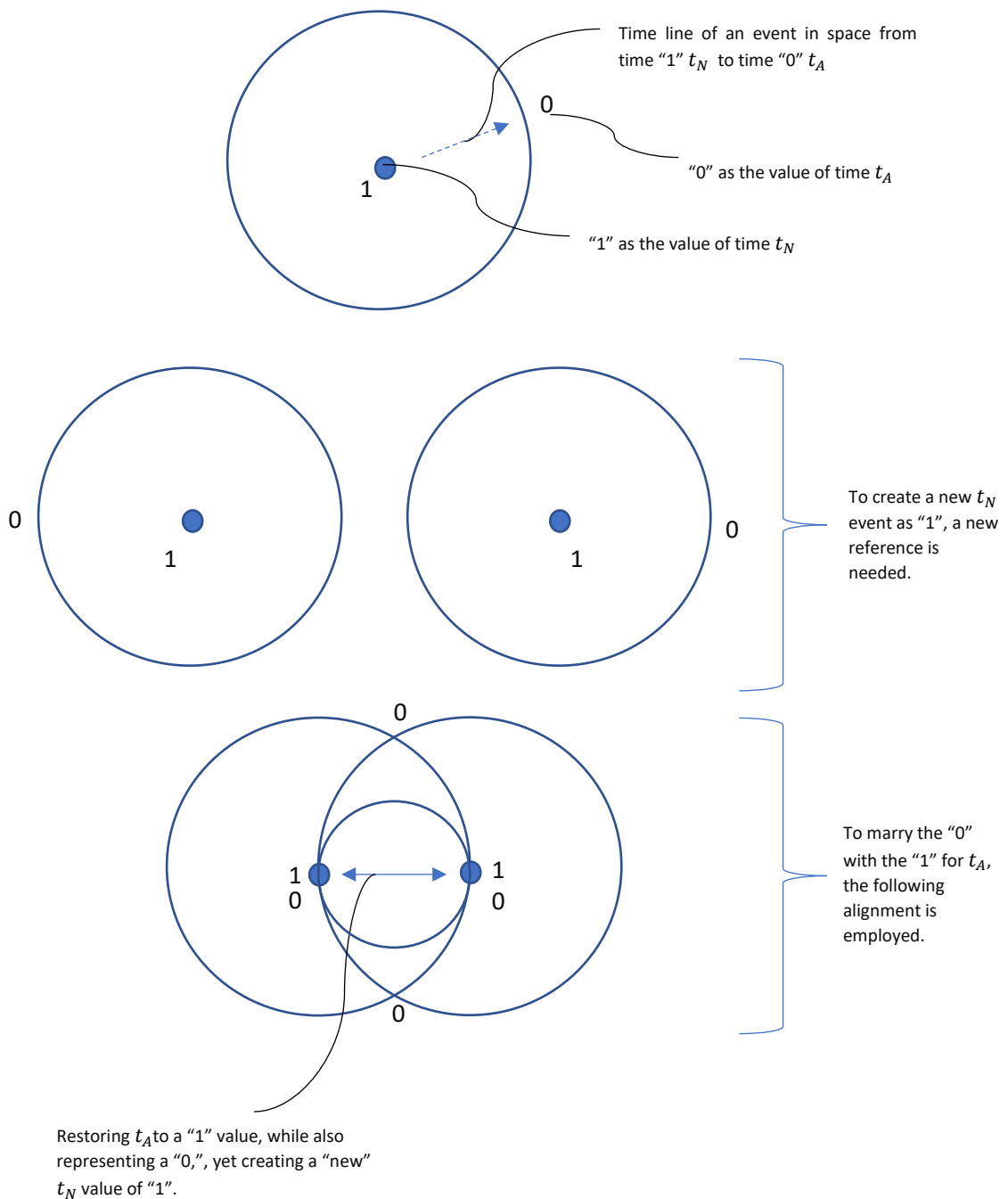


**Figure 2:** schematic description for resolving equations 1-5.

The restoration of  $t_A$  to a "1" value requires "two"  $t_N$  events shown diagrammatically in figure 2. The implication of time  $t_N$  to time  $t_A$  is almost suggesting a movement backwards, from 1 to 0, which despite being a paradoxical feature is explainable; the key implication here is that for gravity as  $t_A$ , gravity is both "1" as time and "0" as time, suggesting  $t_A$  as a value of "1" is itself a  $t_N$  event, a "now" event, and as a feature of "0", as per the description of space in paper 2 ([2]; p4-6), it is also related to "0-scalar" space. In other words, gravity would be an "immediate" field force effect. Further to this though, associated to this immediate field effect would be the idea of energy, as an

extra “1” value for  $t_N$ , as per equation 5. This extra energy of  $t_N$  would though be associated to  $t_A$  as gravity. The other suggestion here therefore is that a “dual”  $t_N$  event is created and thus a type of “splitting” process with a release of energy and with what would appear to be “thrust” (gravitational energy); perhaps to describe this more accurately would be to present the notion of quantum entanglement, which of course in previous papers [4][5][6] has been widely explained in the vein of the relationship between  $\varphi$  and  $\frac{-1}{\varphi}$ . Yet here, we have a process of time approaching a very small number as  $t_A$ , and thus what can only be considered as a very “rapid” event/phenomena.

In further considering the idea of gravity emerging from EM, as per equation 4, gravity would manifest in relation to its value as  $\left(\frac{-1}{\varphi}\right)^2$  as  $t_N$  as a spherical time “front” as explained in paper 2 ([2]; p6); the idea of gravity would exist perpendicular to this  $\left(\frac{-1}{\varphi}\right)^2$  electrical time front, and thus exist along the field line of magnetism, and thus abide by the behaviour of “mass” ( $\varphi$ ). This is of course how gravity behaves, along the line of mass, and how it has been suggested to move here, to operate here as a field force effect, namely as a “magnetic” feature as per paper 4 ([4]; p7-8).

Two features though become apparent, the first is the generation of energy at  $t_N$ , the second is a gravity effect “in a future time-zone”,  $t_A$ , which in itself is unique; it means first would come the energy built up to a  $t_N = 1 + 1$  level, then at that level of  $t_N$  for whatever nominated process would come the gravity effect as  $t_A = 1$ . Simply, as soon as that EM resonance (destructive interference) reaches the level of  $t_N = 1 + 1$  almost immediately would there be a gravity effect as though  $t_N$  (as “1”), and with mass involved this would represent what would appear to be “explosive (high energy and fast) gravitational thrust”.

The question now is how to demonstrate the feature of quantum-gravity in a laboratory and thus how we would create a folded (destructive interference) EM gradient to demonstrate this explosive high energy fast thrust; the most basic suggestion here is creating an electrical solenoid magnet wound back on itself to give rise to a standing magnetic field (destructive interference). The question is, “*according to what scale of winding and electrical field effect, and what type of energy release will be noticed given the equations suggest an almost “immediate”  $t_N$  energy effect yet delayed  $t_A$  gravity effect?*”

#### 4. TESTING EMERGENT GRAVITY

The key idea here is to mimic emergence processes of the atom onto a larger scale, presumably keeping everything in proportion (fractal topology, ([1]; p.19); the theory presented in the preceding 6 papers [1][2][3][4][5][6] highlights the feature of a “fractal” ([1]; p.19) atomic pattern per the golden ratio which suggests we could step up the atom to a basic research-based workable level, and so in doing this we could demonstrate the gravitational features of that stepped up atomic model. This “stepped-up” atom would be the first step in realizing how we can develop a gravitational field based upon an atomic fractal stepped-up basis. In remaining true therefore to the basic scaling of the atom, let’s say we replicate the atomic dimensions in mimicking a fractal stepped-up phi-quantum wave-function as an “ideal” (between positive and negative phi-quantum wave-function atomic charged poles) wave-function length and associated scaling as follows:

- To achieve the fractal stepping-up process, a key fundamental equation needs to be acknowledged, namely the fine structure constant equation for the atom, as follows:

$$\lambda = 2\pi \cdot \alpha \cdot a_0 \quad (6)$$

- Here,  $\alpha$  is the fine structure constant of the atom (a value of  $\sim 1/137$ , symbolic of the strength of atomic electromagnetic coupling),  $\lambda$  the Compton wavelength (electromagnetic wavelength of a basic quanta

regarding the proton (p) and electron (e) atomic construct), and  $a_0$  the radius of the atom (as the distance that separates the proton (p) and electron (e)).

- When we step this equation up fractally to a workable level, not losing the scale of dimensions, the following equations become effective:

$$\lambda_f = \frac{\Omega_f}{21.8} \quad (7)$$

$$\Omega_f = 21.8 \cdot \lambda_f \quad (8)$$

- Here  $\lambda_f$  is the fractally stepped-up value of the wavelength of electrical current (alternating or pulsing) and the solenoid wind-length, and  $\Omega_f$  the distance between a positive and negative charged plate/region;
  - As a wire analogy, there would be ~21.8 winds of a solenoid, which is then wound back on itself with a wavelength of current that meets the description of the dimension of the wind-length (solenoid wavelength).
- Let us consider this equation (eq. 8) as the “gravielectric field equation” which is considered to represent, in incorporating the fine structure constant ( $\alpha$ ), a universal equation applying to all scales of wavelength ( $\lambda_f$ ) and distance ( $\Omega_f$ ) and thus not to the atom alone.
- It can be granted that the “charges” of the electron and proton would be intrinsic to the phi-quantum wave-function delivery, precursory for EM generation, and so for the purposes of the testing here the idea of the field equation can be replaced with an RF source (microwave) fed into a chamber or aerial system without strict attention to the need for a certain number of winds/wavelengths, although there is no harm in accommodating for the gravielectric field equation nonetheless.
- Let us consider a device that utilises this process of EM resonance destructive interference as “gravielectric field generator” which could currently for the purposes of the proposed testing here represent two basic possibilities, a resonant chamber EXPERIMENT 1 (EX-1) fig. 3, or a solenoid/wire system EXPERIMENT 2 (EX-2) fig. 4.
  - **EX-1:** a resonant chamber of 1130MM in length 74MM ID (9a.), that creates a resonant field in the chamber which would contain a tapered rod (5a.) that produces an ideal resonance (destructive field interference, ~25.6MM) at the more massive end of the tapered steel rod (4a.).

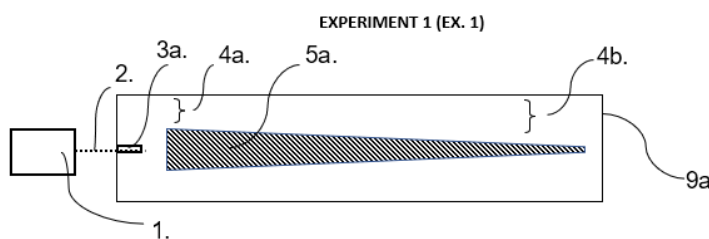


**Figure 3: EX-1;** AC/pulsing power supply for solenoids (1.), connecting coaxial lead (2.), chamber coupling pin (3a.), chamber ideal circumferential distance 25.8mm (4a.), chamber non-ideal circumferential distance ~31mm (4b.), internal steel rod tapered from 22.3mm diameter to 12mm diameter (5a.), aluminium tube cavity chamber 74mm ID (9a.).

- **EX-2:** a rod (5b.) that fits partially within a dual solenoid structure of 25.6MM wind diameter (6a-b., 8.), in a 51.7MM ID resonance chamber (9b.) which fits within the 74MM ID (9a.) general resonance chamber.

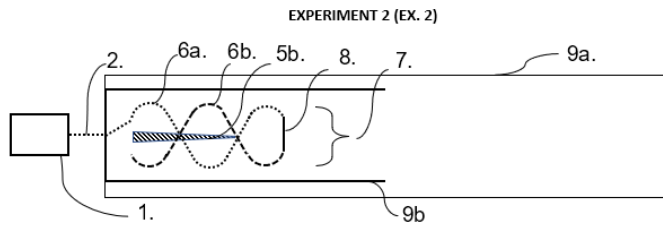


**Figure 4: EX-2;** AC/pulsing power supply for solenoids (1.), connecting coaxial lead (2.), one solenoid (6a.), another solenoid (6b.), solenoid core rod (5b.), solenoid wind diameter (7.), wire joining solenoids at one end (8.), aluminium tube cavity chamber 74MM ID (9a.), inner aluminium tube cavity chamber 51.7MM ID (9b.)

Table 1, figure 5, and images 1-10 are a general overview of the testing parameters and materials.

**TABLE 1**

CAVITY MAGNETRON GENERATOR TESTING: EXPERIMENTS 1 & 2 (EX-1/2)		
EMERGENT ENERGY SCALING:	EM ( $\varphi$ )	GRAVITY( $-\frac{1}{\varphi}$ ) <sup>2</sup>
VALUE:	1.616	0.38
PERCENTAGE COMPARISON:	~80%	~20%
RF POWER OUTPUT:	~400W	
EXPECTED LOSS	~90%	
EXPECTED FIELD OUTPUT	~40W	
( $-\frac{1}{\varphi}$ ) <sup>2</sup> ENERGY SCALED OUTPUT	~8W (20% of 20W)	
<b>POTENTIAL THRUST RESULT:</b>	Power = $M \frac{d^2}{t^3}$	
	For a 5kg mass over a 1s RF field compression exposure:	
	$4 = 5 \frac{d^2}{1}$	
	d = ~0.9 m over 1 second.	
<b>MATERIALS:</b>		
-	800W 5.8 GHz magnetron air cooled, Universal magnetron launcher and WR159 transition waveguide to N-type female connector (UML-TW), EX-1/2, image 1.	
-	N-type coaxial cable male connector to female bulkhead and cap connector, 2m (EX-1), 1m (EX-2), image 2.	
-	74mm inner diameter 113cm long aluminum tube, closed each end with aluminum caps, EX-1/2, image 3.	
-	1000mm long, 22.3mm diameter to 10mm diameter steel rod, EX-1, image 4.	
-	Inner resonance chamber, EX-2, image 5.	
-	Inner solenoid aerial system, EX-2, image 6.	
-	Inner solenoid aerial system rod, EX-2, image 7.	
-	Inner resonance chamber-aerial and rod, EX-2, image 8.	
-	Suspension device (swivel arm and spring), EX-1/2, image 9.	
-	measurement-instrument, EX-1/2, image 10, figure 5.	
-	JVC FULL-HD video recorder.	



Image 1.



Image 5.



Image 6.



Image 2.

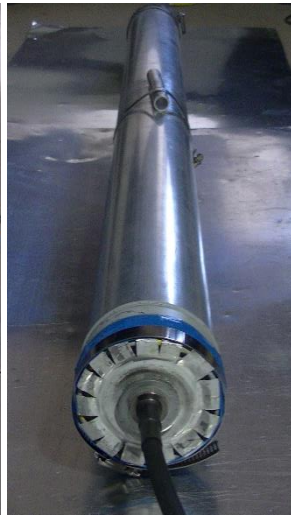


Image 3.



Image 4.



Image 9.



Image 7.



Image 8.

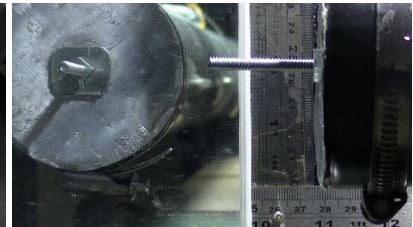
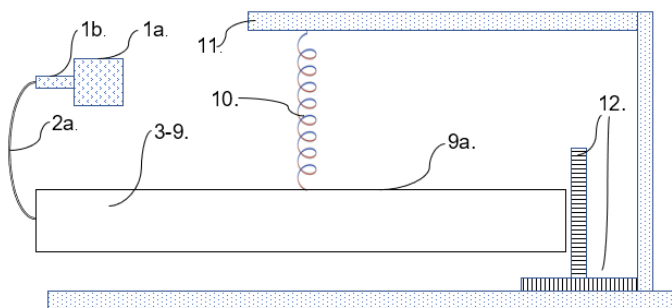


Image 10.



**Figure 5:** 800W 5.8 GHz magnetron AIR-COOLED (1a), Universal magnetron launcher and WR159 transition waveguide to N-type female connector (UML-TW) (1b.), 1m-2m coaxial cable with N-type male connector to N-type female bulkhead (2a.), internal aerial system (3-9.), 74MM ID 1130MM long aluminum cavity tube (9a.), Aluminum tube suspended horizontally from swivel-arm (11.) by spring (10.), measurement rulers to measure movement at the distal end of resonance cavity tube (12.)

As per the above description of EM resonance generation there are two options:

- the first is in using a cavity chamber and resonance abiding by the gravielectric field equation,
- the second is in using an antenna/wires as solenoids in the cavity chamber of arbitrary length and aerial of arbitrary solenoid wind number, yet still with the focus on creating the correct destructive interference resonance, despite “how long” that field would be in distance, and thus abiding by the right solenoid wind diameter.

The problem with using wires in the cavity chamber to effect an EM resonance (destructive interference) is the energy loss along any such solenoid at such a high frequency, and thus field-signal integrity loss; abiding by the gravielectric field equation would not (and did not in testing) yield fruitful results. The following two testing procedures explain what was “found” as what **could** be interpreted as a **positive result for emergent quantum gravity**, as the “best” results gained through a vast number of testing profiles, results from a number of different experiments with

various configurations of rod and solenoid design, only though documenting here what has yielded results and the explanation as to more than likely why those results were yielded.

#### 4.1 EXPERIMENT 1 (EX-1).

In going for the most efficient form of microwave field propagation and thus maximising efficiency, a pure cavity containing the graded rod with the RF field supplied by a free antenna inside the microwave chamber was employed; once again note that the thinking here is that the tapered rod itself as per its dimension/shape by design would act as a way to resonate the field against the surrounding aluminium chamber wall more cleanly at the greater mass-end of the tapered rod (fig. 3).

The idea here is not using any wires as per how to most efficiently set up an EM gradient, namely that the field needs to be allowed to resonate in a tapered fashion and thus needing a certain tapered cavity diameter, as described per the use of a tapered inner rod. The take home message regarding the microwave cavity chamber is that the folded EM field needs to resonate freely in the chamber, and when allowed to would produce thrust from a region of less EM folding (destructive interference) to greater EM folding (destructive interference), a “specific” process that aims to adhere to the fundamental elementary particle scaling of the phi-quantum wave-function atom as a “gradient” (lesser to greater) concentration of harmonic (folded-over, out of phase) EM field, a field that utilizes the entropic features of energy related to the force of gravity. Figure 6 highlights how this most simply would work, where the area of darker shading represents a greater concentration of folded/harmonic (destructive interference) EM field, and the associated thrust is represented by the blue arrow.



**Figure 6: EX-1** (see previous figure descriptors for EX-1); blue arrows as direction of thrust.

Now we would need to measure the motion of this system with RF activation. The idea proposed here is to suspend the chamber from a spring such that the antenna device is at one end of the suspended device, and thus the antenna mechanism representing itself around a fulcrum point of movement which would then, if movement exists, result in either end displaying movement around the suspension centre region, as per figure 6-7.

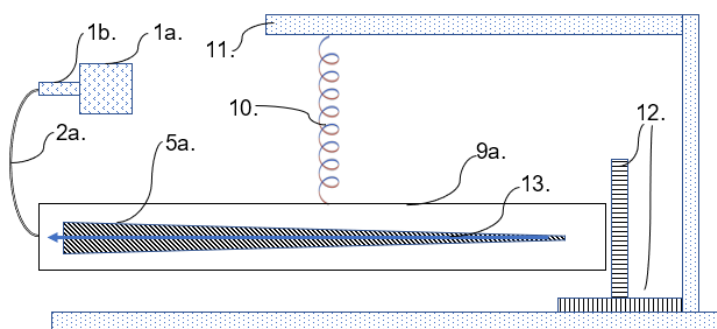


**Figure 7:** 800W 5.8 GHz magnetron AIR-COOLED (1a), Universal magnetron launcher and WR159 transition waveguide to N-type female connector (UML-TW) (1b.), 2m coaxial cable with N-type male connector to N-type female bulkhead (2a.), internal aerial system (3-9.), 74MM ID 1130MM long aluminum cavity tube (9a.), Aluminum tube suspended horizontally from swivel-arm (11.) by spring (10.), measurement rulers to measure movement at the distal end (12.), blue arrow anticipated direction of movement (13.)

The result here was interesting; the antenna pin in the magnetron launcher chamber jettisoned out like a bullet from a gun, almost puncturing a hole in the aluminum transition wave-guide wall structure (which required re-tooling/shaping). The first impression was that there was “arcing” in the coaxial connector at the aluminum wave-guide site, despite there being no reason for the arcing to take place at that location as per previous experiments,

and no reason for that exact nature of repeated jettison/propulsion of the pin compared to a large number of other tests albeit different configurations. The following figures (fig 8., fig 9.) and pictures (images 1-6) highlight this effect:

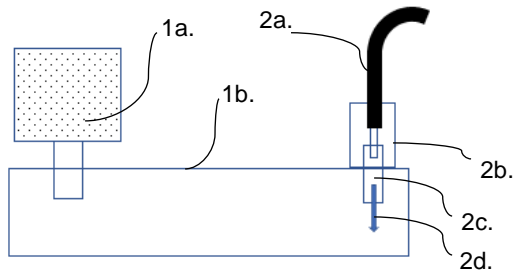


**Figure 8: EX-1;** 800W 5.8 GHz magnetron AIR-COOLED (1a), Universal magnetron launcher and WR159 transition waveguide to N-type female connector (UML-TW) (1b.), 2m coaxial cable with N-type male connector to N-type female bulkhead (2a.), N-type female bulkhead (2b.), coupling pin (2c.), direction of thrust of coupling pin (2d.)

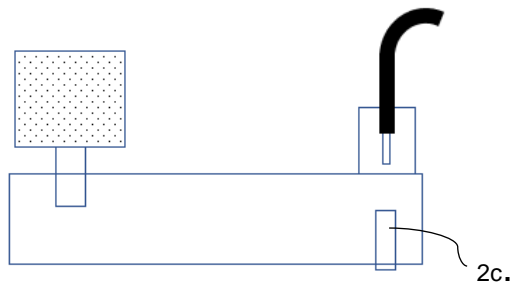


**Figure 9: EX-1;** detached coupling pin (2c.)



Image 11.



Image 12.



Image 13.



Image 14.

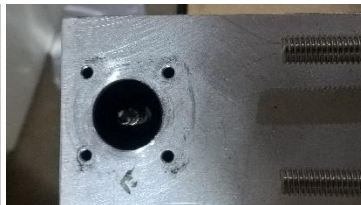


Image 15.

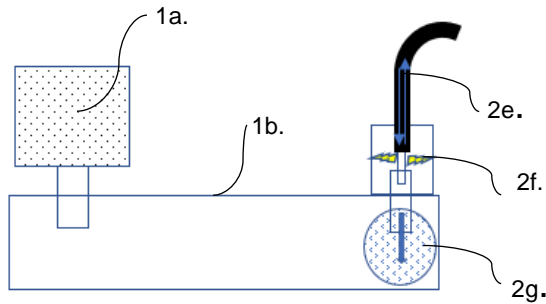


Image 16.

**Images 11-16:** Image 11 represents a standard intact N-type female bulkhead and coupling pin, Images 12-13 represents the N-type female bulkhead with pin detached (expelled), Image 14 represents the expelled pin, Image 15 is how the expelled pin appeared on removal of the female bulkhead, Image 16 represents the Universal magnetron launcher and WR159 transition waveguide to N-type connector (UML-TW) highlighting a central impression from the expelled pin.

This experiment was repeated numerous times with the same result, ultimately abandoned given its destructive nature to the research equipment. The issue encountered was initially thought to be a result of a great buildup of energy close to the aluminum transition wave-guide in the coaxial connector, creating a type of arcing it would seem, somehow enforcing what would appear to have been a projectile effect in the firmly placed antenna pin outwards into the magnetron launcher system. Many tests were run with this configuration and other configurations, and only this configuration had the projectile response (and associated buildup of energy, as it can only be assumed, leading to the expression of force in the pin). The only “other” explanation for the projectile effect (as other tests ran with different configurations resulted in arcing yet not this projectile response) was that there was a “great” EM

destructive interference feedback taking place in the gravielectric field chamber, feeding back into the coaxial cable from the larger gravielectric field chamber, back into the magnetron launcher, creating a folded (destructive interference) EM wave of greatest intensity in the aluminum transition wave-guide central to the aerial pin inside the aluminum transition wave-guide, enforcing the pin as a “mass” to **project** into the region of greatest spatial compression (EM folding, destructive interference):



**Figure 10:** EX-1; 800W 5.8 GHz magnetron AIR-COOLED (1a), Universal magnetron launcher and WR159 transition waveguide to N-type female connector (UML-TW) (1b.), proposed resonance field effect in coaxial cable (2e.), proposed arcing in female bulkhead cavity (2f.), proposed region of EM resonance field in magnetron launcher (2g.)

Once again, the explanation here with this effect is that the possibility exists according to this theory that the field had reflected up the coaxial wire owing to a stronger resonance closer to the chamber aerial, and this somehow created a resonant field in the region of the pin itself in the launcher chamber, creating gravitational thrust in the pin to such a level it jettisoned into the magnetron launcher. Why **into** the magnetron launcher? Further to this, why did not the antenna pin in the gravielectric field chamber (greater chamber) jettison out as well like as what happened in images 11-16?

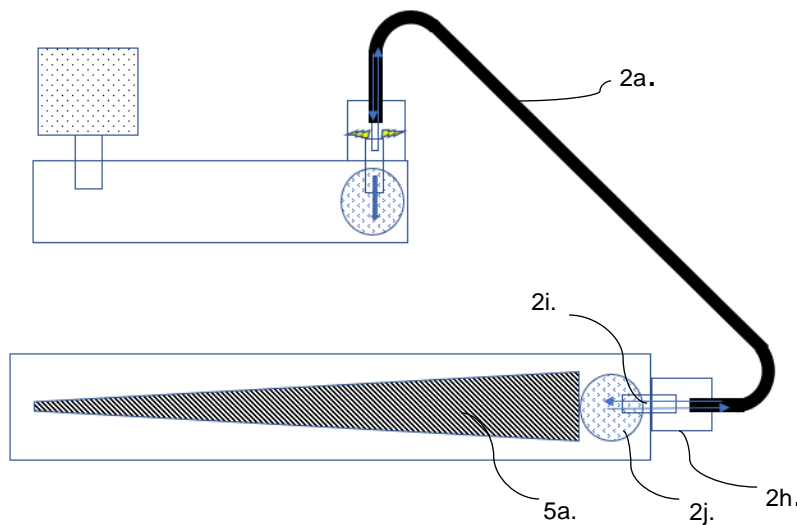


**Figure 11:** EX.1; 2m coaxial cable with N-type male connector to N-type female bulkhead (2a.), N-type female bulkhead (2h.), gravielectric chamber coupling pin (2i.), proposed EM resonance field region (2d.), internal steel rod tapered from 22.3mm diameter to 12mm diameter (5a.)

The thinking is that the resonance field is, by this configuration, stronger/more-intact/purer in the aluminum transition wave-guide than the gravielectric field chamber, hence the pin in the aluminum transition wave-guide being the obvious weakest link, yielding to what it seems to be a perfect destructive interference resonance field zone, a perfect destructive EM resonance field area, jettisoning into it. With all such considerations, the task thus was to create a stronger EM destructive resonance in gravielectric field chamber using an aerial structure that could better harness the destructive resonance EM field, more than in aluminum transition wave-guide, and thus somehow prevent EM feedback along the coaxial cable into aluminum transition wave-guide system, while creating a type of deliberate coupling pin (aerial) structure in the gravielectric field chamber to effect an overall propulsion of the chamber structure itself like the magnetron launcher coupling pin.

4.2 EXPERIMENT 2 (EX-2).

The aim here is to keep the resonance in the gravior electric field chamber as per a discharge of energy there in that chamber, not near the magnetron launcher chamber, yet a bleeding of energy into the greater chamber; the idea here is to create an independent EM destructive interference field (to satisfy equation 4) within the large EM-chamber (1130mm length enclosed aluminum tube), with particular attention to the right scale of solenoid-constructed destructive interference resonance wind diameter. The best way to do this would be to create a solenoid as an antenna that creates the same effect as an EM resonance field of the value we seek.

In breaking this down, take a field, the proposed EM resonant field as follows as generated by a solenoid, as per figure 1.

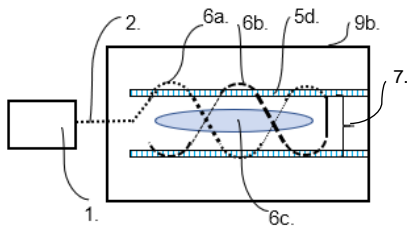


**Figure 12:** RF source (1.), connecting coaxial lead (2.), one solenoid (6a.) ~5 winds forward (image 7), another solenoid (6b.) ~5 winds back (image 7), solenoid winding Perspex tube bulkhead (5d.) attached to 51.7mm ID aluminium pipe structure (9b.), EM destructive-interference field region (6c.), solenoid wind diameter 25.8mm (7.), see images 6-9.

Then we would place a mass in that field attached to the chamber bulkhead as per figure 2, much like the coupling pin (2c.) in the magnetron launcher (1b.).

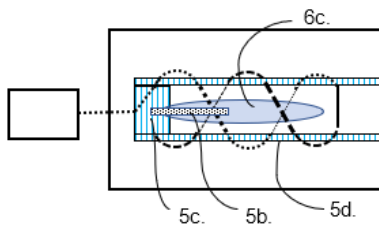


**Figure 13:** Perspex rod bulkhead (5c.) attached to Perspex tube bulkhead (5d.), rod (5b.), see image 8, exposed to EM resonant field (6c.)

In placing that mass in the centre of that field, that mass according to this theory would try to move into that field, in being attracted by it. Also associated to this field would be the creation of energy, electrical energy perpendicular to that EM destructive interference field. A variety of rods were used, ranging from Perspex, to steel, to silver. Given that an ideal resonance (as per a folded destructive interference EM field) was required, a new inner tubing system had to be crafted for this new aerial system as per images 5-8 (p8).

Now we would need to measure the motion of during RF activation; the idea proposed here is to once again suspend the chamber from a spring such that the antenna device is at one end of the suspended device, and thus the antenna mechanism representing itself around a fulcrum point of movement which would then, if movement exists, result in either end displaying movement around the suspension centre region, as per figure 14.

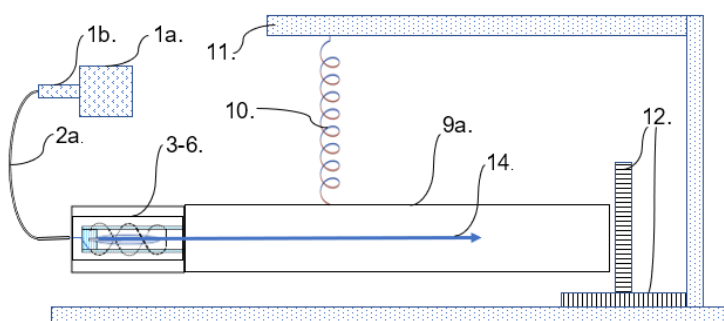


**Figure 14:** 800W 5.8 GHz magnetron AIR-COOLED (1a), Universal magnetron launcher and WR159 transition waveguide to N-type female connector (UML-TW) (1b.), 1m coaxial cable with N-type male connector to N-type female bulkhead (2a.), internal aerial system (3-6.), 74MM ID 1130MM long aluminum cavity tube (9a.), Aluminum tube suspended horizontally from swivel-arm (11.) by spring (10.), measurement rulers to measure movement at the distal end (12.), anticipated direction of thrust/movement (14.)

Once again, the idea here is to create an independent EM destructive interference field within the chamber, with particular attention to the right scale of the EM phi-quantum wave-function destructive interference, and to then have the rod in the chamber yield itself into that EM destructive interference field and thus effect movement of the associated attached bulkhead in that same direction.

The results gained were nothing short of explosive as per the two key tests performed with the configuration described ([14]; <https://www.youtube.com/watch?v=KbQxy8klS-8>). The anticipated thrust and associated direction were achieved, however owing to the limitation of the structural parameters of the test, the chamber broke down as the safety chamber connectors became detached at the aerial end, as per tests EX-2.1 and EX-2.2 highlighted in the video. Given the sudden thrust achieved, the initial impression was that an “explosive” process was at play through perhaps massive arcing of the antenna in the chamber igniting something. The problem here though is that through all the other tests performed, far more arcing had been noticed through various parts of the antenna system without any thrust, just Perspex melting and associated smoke from the arcing through the Perspex bulkheads. Here in these two tests the main arcing appears to have taken place within the N-type male plug (image 17) and insulating material (image 18) causing a separation, sudden and forceful, at the safety separation plug (image 19), resulting in images 20-22 which show the movement of the insulating N-type male connector insulating material (image 20), the post-test removed pin and insulating material from the plug (image 21), and a post-test cut-away version of the insulating material showing what appears to have been arcing (image 22).



Image 17



Image 18



Image 19



Image 20



Image 21

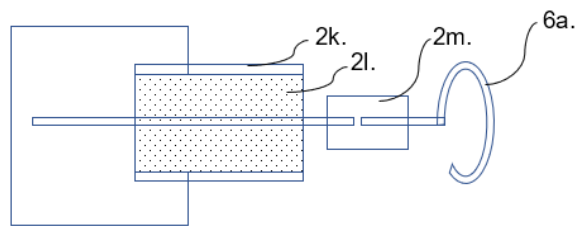


Image 22

**Images 17-22:** **Image 17** represents a standard intact N-type male connector, **Image 18** the coaxial insulating material between the N-type male connector and aerial copper wire, **Image 19** represents a safety disconnection plug in the event of rapid thrust, **Image 20** represents what was viewed at the aerial plug end after experiments 2.1 and 2.2, namely the aerial separating at the safety disconnection plug socket, **Image 21** shows the removed aerial with insulating material (from the N-type male connector), **Image 22** shows a cut-away of the insulating material highlighting what appears to have been a combustion (high energy) process taking place, albeit in a very small pocket of insulating material.

This arcing has been noticed in previous tests without any of the propulsion, albeit due to a different configuration (namely not using the internal 51.7MM ID chamber). It became evident nonetheless that combing the aerial with the 51.7MM ID chamber yielded thrust detailing not just propulsion yet energy along with this propulsion. To note is that the part of the aerial in question (with insulating material) did not completely disintegrate, nor was itself (insulating material) blown out of the male N-type connector, as per image 20. This suggests that the propulsion at play could have come from another source, namely the idea as presented in figures 15-16.

BEFORE RF-EXECUTION



**Figure 15:** male N-type connector (2k., image 17), male N-type connector insulator (2l., image 18), antenna safety plug (2m., image 20), internal solenoid (6a, image 6)

DURING/AFTER RF-EXECUTION

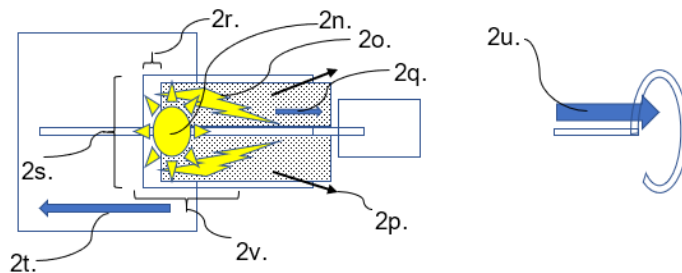


**Figure 16:** internal combustion region (2n., image 22), combustion development along internal insulator (2o., image 22), proposed leak of combustion material between N-type male connector and N-type male insulator (2p.), direction of movement of N-type male insulating material (2q.), gap created by movement of N-type male insulating material in N-type plug (2r.), ~7mm diameter of gap (2s.), proposed movement of N-type male plug (2t.), proposed movement of antenna from antenna safety valve (2u.) by the proposed effect of the destructive interference EM field.

Here, one proposed explanation is that there would have been an explosion (2n., 2o.) leading to a rapid release of gas (2p.) as evident by the forward motion of the insulating material (2q., 2r.) leading to a reaction of the cap at the RF entry end of the chamber (2t.) having an overall propulsive reactive effect forward of the overall chamber (2u.) that became detached from the RF entry cap area of the chamber, as per figures 15-16.

Although that appears good in theory, the amount of thrust demonstrated and the very small space involved at this apparent arcing site (~3-4 mm<sup>3</sup> of cable insulating material vaporized) and the time it took for this to happen (~4s following RF activation) does suggest more could be going on hence the proposed “2u.” effect, as per the destructive interference EM resonance field. There is also the possibility that the fluctuating sparking in regions 2n. and 2o. could have had a type of “magnification” effect (like a Tesla coil) in the aerial system (6a.), leading to what appeared to have been a step-up of voltage for the resonance field to be effected (fig. 13, 6c.), playing out figure 14, which as an event of energy release would be quite sudden as per the theory ( $t_N$  as “1” and  $t_A$  as “0” and “1”).

Only further testing in being able to witness the inner workings of the chamber during RF activation could provide any indication. It is important to note though that the same result was yielded to the normally very well held coupling pin in EX-1, and indeed what type of force would be required to have a firmly bound coupling pin jettison out of its socket without much apparent distress to its underlying coaxial bulkhead housing structure. Here we have been able to mimic the same effect in the resonance chamber with a similar result, while in both cases “more” seeming to be responsible for the results gained than mere arcing alone; the important thing to note is the “suddenness” of the movement, the suggestion being here of an apparent compression of time as energy as gravity, yielding a “projectile” effect of the mass involved, as the golden-ratio equations for time regarding emergent gravity would hold.

With all such considerations, in the absence of any contemporary explanations for the phenomena, and in light of the primary theory leading to this testing process, it is considered that the results here are a step towards highlighting that it *could* indeed be possible to generate a gravity field from EM, and to thus generate gravitational thrust from the effect of an EM resonance (destructive interference) field, despite how unpredictable owing to the current experiment/test parameters. Future research will aim to present mechanisms that appropriate cleaner and

more observable results (within the chamber), with the aim of granting greater certainty to the theory behind the research and associated results; to note once again, EX-2 had to be shut down after two runs (despite doing a large number of other runs with different configurations without the explosive result yielded in the EX-2 configuration described) owing to the counterproductive nature of the results to the structural integrity of the research equipment used. It is thus considered that further testing is warranted with attention to measuring/monitoring the nature of the phenomena inside the chamber during RF application with the aim of better accommodating for the sudden high energy thrust.

In short, the provisional results here were achieved in employing a RF fed aerial design into a closed aluminium chamber, affecting what appears to be a high energy projectile effect within the chamber central to the resonant (EM destructive interference) field. The results are considered provisional as they compromised the boundaries of the testing structural framework thus warranting the need for further and yet more structured testing, results that are considered nonetheless by comparison to previous testing parameters to be noteworthy.

#### 4.3 CONTEMPORARY EFFORTS (EM-DRIVE RESEARCH)

The question now beckons, “does other research exist for EM warp/gravity drive and what are those findings?” It does, as per EmDrive research [15][16][17][18][19][20], heralded as a propellant-free drive which, much to the criticism of the scientific community, would have to violate both conservation of momentum and conservation of energy in order to work. Such devices and research allegedly produces thrust from an electromagnetic field inside a cavity, without ejecting mass, per a type of radiation differential of pressure in the chamber (the current explanation used). Several prototypes have been constructed and tested (figure 17), including by Eagleworks, the Advanced Propulsion Physics Laboratory at NASA. As of 2017, a few tests of prototype drives were reported to produce a small apparent thrust [21] while other prototype tests did not report any thrust.

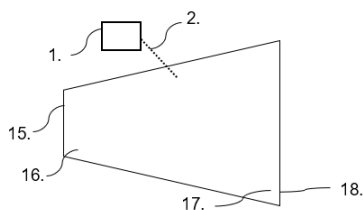


**Figure 17:** Conventional EM thruster; magnetron microwave source (1.), attachment/coaxial cable (2.), smaller diameter end of vacuum chamber cavity (15.), obtuse angle between smaller cavity end and tapered cavity wall (16.), acute angle between larger cavity end and cavity wall (17.), larger diameter end of cavity (18.)

In explaining the physics of propulsion here using the phi-quantum wave-function and associated destructive interference resonance requirement, here, instead of using a structure that yields an ideal destructive interference resonance, we’re using the idea of “angles” to “disturb” an ideal resonance, an ideal resonance that in this configuration of the chamber would be largely hit and miss; as the angles of this chamber would represent a “disturbance” to an ideal resonance, there is “more disturbance” at the greater-diameter end of the cavity than the smaller end of the cavity, and thus less of an EM resonance (destructive interference) field at the larger diameter end. Simply, we have an acute angle at one end of the chamber for the field to be disturbed from an ideal resonance, to bounce between (a lowest chance of resonance in this configuration owing to the greater area of angle), and an obtuse angle at the other end of the container/cavity (a not as low chance of resonance in this configuration owing to the less area of angle), simply because the region of greatest disturbance to an ideal resonance would be the larger region holding that unideal field reflection. Thus, the thrust anticipated here would be according to figure 18, from a region of greatest disturbance of an ideal EM resonance (destructive interference) to a region of least disturbance of an ideal EM resonance.

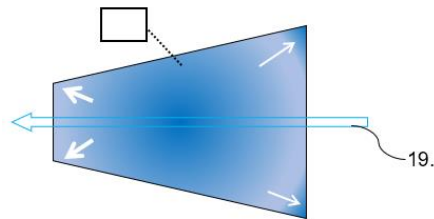


**Figure 18:** Conventional EM thruster (see previous related figure descriptors); theorised direction of thrust (19.).

The thrust here would not be as focused as EX-1/2; the electromechanical set-up would provide no-where near the same efficiency EX-1/2 would, as EX-1/2 accommodates for the actual destructive interference resonance of the microwave field ideally “entire”, whereas here the resonance depends on the obtuse angle of the chamber to not be as disruptive as the acute-angle region in disturbing an idea EM resonance. Note though that arcing would still form in this configuration, and thus overheat the system, despite a vacuum chamber being used or not. Suffice to say, any such research that avoids considering the actual entropic processes for gravity would have a great blind-side on how the research would evolve as a technology, how it would be disputed, and furthermore how it would be ultimately put down to other interfering ideas, ideas such as a fault in the chamber itself or associated cables [22][23] being affected by the Earth’s magnetic field. Despite the criticism of contemporary EM thruster research in general, the EM resonance in the cavity chamber would have a limit of energy input usefulness as per the design of the chamber’s angles disturbing an ideal resonance (according to the theory behind the EM thruster presented in this paper). As highlighted in the theory here, of particular note is that current research into EM thrusters, in comparison to the EX-1/2 model, will have limited results owing to it depending mostly on the gradient of disturbance of EM field resonance, from the greatest disturbance of EM destructive interference resonance (large end) to the least disturbance of EM destructive interference resonance (small end); thus, only a small amount of thrust would still ever apparent with a large energy input, if not unnoticeable.

#### 4.4 DISCUSSION OF RESULTS COMPARED TO EM-DRIVE RESEARCH

The following are the key points to be considered from the two experiments (EX-1 and EX-2) compared to current EM-drive research:

- Energy and motion were both generated in EX-1 and EX-2 in using equipment designed not to explode in carrying the specified RF energy, equipment (cables etc) designed to withstand the input RF energy:
  - The amount of energy and motion generated **can** nonetheless be explained with the forwarded theory (the new theory that inspired the intention of research).
    - This amount of energy release and motion is above and beyond that of non-theory parameters.
- Numerous tests (~200) of various configurations of chamber and antenna design were performed using parameters outside those specified for EX-1 and EX-2 without the same motion, only at best generating an “arcing” between the wires of the various types of antennas researched in effecting their redundancy in performance through general RF heat effects in the RF chamber and on associated Perspex bulkheads (used to prevent arcing).
- Owing to EX-1 and EX-2 being compromised by the results through their sudden and explosive nature of energy and motion, the experiments should not yet be granted as successful in confirming the theory owing to the breakdown of the research platform by the results:

- EX-1 and EX-2 could be interpreted as mere “explosions”, yet the feature of these explosions and their characteristic nature (in line with the parameters of the gravielectric field equation) warrant further research:
  - The equipment used is designed “not” to explode yet carry the RF input energy
  - Future research needs to focus primarily on EX-2 with the aim of witnessing the energy and motion dynamic within the chamber during RF activation and to better design the internal RF connector and antenna accordingly.
- Current results thus lead to the suspicion that a theory that prompted the testing yielding the results as compared to non-theory parameters yielding practically no results uphold the notion that the gravielectric field theory and testing is worthy of further investigation.

## 5. CONCLUSION

After a running a series of tests, it is considered that further testing is warranted, with attention to measuring/monitoring the nature of the phenomena inside the chamber. In terms of a more precise comparison between contemporary EM-drive research and the specifications of the testing offered here for a resonant chamber, the scaling/comparison between these notions is not in any way too dissimilar; given that gravity and electromagnetism are proposed to be emergent features of this fundamental scaling system, the “emergent” feature of this scaling system can change, in dimension and number of folded wavelengths, in that any number of winds could be used and any type of winding-taper along a solenoid rod without adhering directly to the scaling system. Thus, although fractally stepping up the scale of the atom would provide an “ideal” result, of course any number of destructive interference resonance wavelengths can be used, any gradient of standing destructive interference EM waves, when applied to any type of solenoid length or graded rod. The idea here is the “emergent” feature of gravity and electromagnetism which would not need to adhere to the exact scaling of the elementary particle and phi-quantum wave-function scaling system, although adhering to the “exact” scaling **could** be an ideal result.

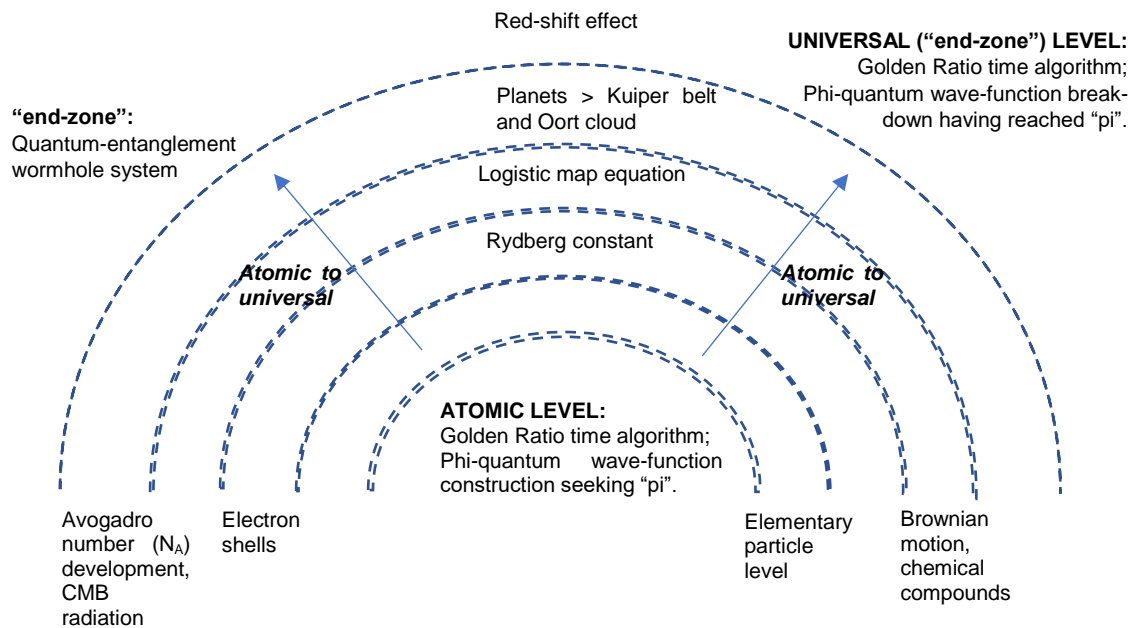
The aim with this paper and previous papers [1-6] is to give the proposed golden ratio algorithm for time an exhaustive look into; the quest here is to present a reproducible laboratory feature that contemporary ideas of time and space cannot predict/explain by the manner of their current definition of “time” and associated research pathways. It cannot be stressed enough that “only” the physical data that is trusted from tried and tested research has been applied to this new a-priori for time (and space) in all the papers leading to this one, in “**better joining**” known tried and tested equations for mass, energy, gravity, electromagnetism, including known scales of weights and measures thereof using this new algorithm for time. Table 2 lists the tried and tested data and their corresponding values to the new algorithm for time, and figures 19-20 provide the overall scope of the new algorithm for time and associated wave-function throughout theoretical space. Note that the only feature that links all the relevant equations is the new algorithm for time and associated phi-quantum wave-function. Note also that the fundamental derived constant is the fine structure constant; when values of mass and charge and the radial dimension of the atom are applied to this theorized value of the fine structure constant, all other values fall into place applicable to gravity and electromagnetism and the associated wave-function for light, from which the strong ([4], p.7-8) and weak ([4]; p.10) nuclear forces become apparent and can be explained accordingly in this new context.

TABLE 2

<ul style="list-style-type: none"> <li>• <u>THE FUNDAMENTAL DERIVED CONSTANT IS FOR THE PHI-QUANTUM WAVE-FUNCTION:</u> <ul style="list-style-type: none"> <li>○ 21.8 phi-quantum wave-function units between the theorized electron and proton.</li> <li>○ When this value is applied to the idea of a basic wavelength of an atom, the following is achieved:           <ul style="list-style-type: none"> <li>▪ <math>\lambda = \frac{a^0}{22}</math>, thence <math>\frac{\lambda}{2\pi} = \frac{a^0}{2\pi \cdot 21.8} = \frac{a^0}{137}</math></li> </ul> </li> </ul> </li> <li>• <u>WHEN VALUES OF MASS AND CHARGE AND THE RADIAL DIMENSION OF THE ATOM ARE APPLIED TO THIS THEORIZED VALUE OF THE FINE STRUCTURE CONSTANT, ALL OTHER VALUES CAN BE DERIVED USING THE PHI-QUANTUM WAVE-FUNCTION, INCLUDING THE FOLLOWING:</u> <ul style="list-style-type: none"> <li>○ <math>\frac{19.8 \cdot \lambda}{e_c} = \frac{19.8 \cdot 2.426 \cdot 10^{-12}}{1.60218 \cdot 10^{-19}} = 2.998 \cdot 10^8 \text{ ms}^{-1}</math></li> <li>○ <math>e_c = \frac{19.8 \cdot \lambda}{c}</math></li> </ul> </li> <li>• <u>USING THE TIME ALGORITHM RESULTS IN THE BASIC EQUATION FOR ELECTROSTATIC FORCE:</u> <ul style="list-style-type: none"> <li>○ <math>Q_{AB&lt;NEWTONS&gt;} = \frac{Q_C c^2 Q_A Q_B}{d_{AB} d_{BA}} (C^3 t^{-2})</math> whereby <math>Q_C c^2 = k_e</math></li> <li>○ Thus, <math>Q_C = \frac{3 \cdot 2e_c}{4\lambda}</math>, thence <math>k_e = \frac{3 \cdot 2e_c}{4\lambda} \cdot c^2 = \frac{6 \cdot 1.6 \cdot 10^{-19} \cdot (3 \cdot 10^8)^2}{4 \cdot 2.426 \cdot 10^{-12}} = 8.9 \cdot 10^9 \text{ Cms}^{-2}</math></li> </ul> </li> <li>• <u>USING THE TIME ALGORITHM RESULTS IN THE BASIC EQUATION FOR GRAVITATIONAL FORCE:</u> <ul style="list-style-type: none"> <li>○ <math>G_{AB&lt;NEWTONS&gt;} = \frac{M_C M_A M_B}{t_{AB} t_{BA}} (kg^3 t^{-2})</math>, thence <math>G_{AB&lt;NEWTONS&gt;} = \frac{M_A c^2 M_A M_B}{d^2} (kg^3 t^{-2})</math></li> <li>○ Thus, <math>M_C = \left(\frac{2}{3}\right)^2 \cdot M_p</math>, thence <math>M_C = 3.33 \cdot 10^{-27} \cdot \frac{2}{3^2} \cong 7.4 \cdot 10^{-28} (kg)</math>, thence <math>M_C c^2 = 7.4 \cdot 10^{-28} \cdot (2.99 \cdot 10^8)^2 \cong 6.67 \cdot 10^{-11} = G (kg d^2 t^{-2})</math></li> </ul> </li> <li>• <u>USING THE TIME ALGORITHM ALSO GIVES RISE TO THE RYDBERG FORMULA FOR THE TIME-STATUS OF THE ELECTRON:</u> <ul style="list-style-type: none"> <li>○ <math>\frac{1}{\lambda} = Z^2 \cdot \frac{1}{\left(\frac{1}{n_1^2}\right) - \left(\frac{1}{n_2^2}\right)} \cdot \frac{\lambda_e}{2(2\pi a_0)^2} = R_\infty Z^2 \cdot \frac{1}{\left(\frac{1}{n_1^2}\right) - \left(\frac{1}{n_2^2}\right)}</math></li> </ul> </li> <li>• <u>A NEW WAVE-FUNCTION FOR LIGHT TERMED THE "PHI-QUANTUM WAVE-FUNCTION" EXPLAINS THE EMERGENCE OF GRAVITY FROM ELECTRODYNAMICS ON THIS LEVEL, TOGETHER WITH DETAILING THE STRONG (section 4.3) AND WEAK (section 4.5) NUCLEAR FORCES AND THE EXISTENCE OF THE ELEMENTARY PARTICLES AND THEIR BASIC INTERACTIONS (SPIN etc.).</u></li> <li>• <u>VIA FURTHER THEORY IN USING THE "PI-ERROR GRADIENT" REGARDING THE PHI-QUANTUM WAVE-FUNCTION, AN APPROXIMATE VALUE FOR THE AVOGADRO NUMBER IS DERIVED (0.8% error):</u> <ul style="list-style-type: none"> <li>○ <math>\frac{\pi \text{ error gradient}}{\text{mass of neutron}} = \frac{1.017 \cdot 10^{-3}}{1.675 \cdot 10^{-27}} = 6.072 \cdot 10^{23}</math></li> <li>○ Thus, <math>\frac{6.072 \cdot 10^{23} \cdot \text{mass of neutron}}{\pi \text{ error gradient}} = 1 \text{ unit of mass}</math>, as <math>\frac{6.022 \cdot 10^{23} \cdot \text{mass of neutron} \cdot k_s}{\pi \text{ error gradient}} = 1 \text{ unit of mass}</math></li> </ul> </li> <li>• <u>WHEN APPLIED TO THE TIME-FUNCTION WE ARRIVE AT A VALUE FOR THE CMB RADIATION EFFECT:</u> <ul style="list-style-type: none"> <li>○ <math>\frac{t_A}{21.8} = \frac{1}{N_A}</math>, thus <math>t_B = \sqrt{\frac{21.8}{N_A}}</math>, thus <math>\sqrt{\frac{21.8}{6.072 \cdot 10^{23}}}</math> which equates to <math>5.99 \cdot 10^{-12} \text{ s}</math>; as a value of <math>s^{-1}</math> we have a value of <math>1.67 \cdot 10^{11} \text{ s}^{-1}</math>, or as we know <math>167 \text{ GHz}</math></li> </ul> </li> </ul>
---

**Table 2:** The key equations linking "known values" to the "phi-quantum wave-function values". The theorized values for the CMB and Avogadro's number would appear to be slightly out compared to observed measurements, yet this minor discrepancy is considered to be a result of a type of system tolerance which harbors a natural amount of error in order to satisfy the prime directive of "time" seeking to define "pi", together with the natural occurrence of "c" violations throughout the entire universal manifold of time-space (owing to the "end-zone" universal quantum-entanglement effect, which would have a natural stretching (approaching infinity) effect on the wave-function, increasing the value of the pi-error gradient ([4]; eq.3, p16), in effect making the calculated value of  $N_A$  here under what it is observed to be.

The overall **local** universal scheme would be as figures 19 and 20.



**Figure 19:** Diagram of the general flow of procedures that time as per the phi-quantum wave-function must undertake to fulfil all its requirements of a-priori definition as the golden-ratio time algorithm.

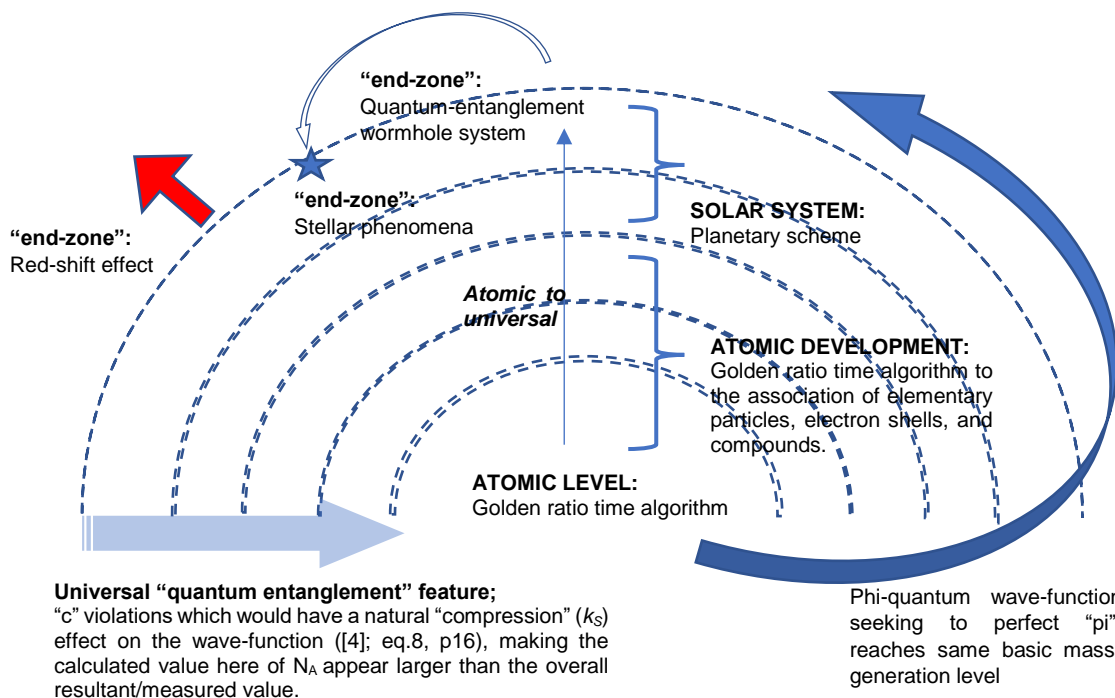


**Figure 20:** A more detailed diagram of the general flow of procedures that time as per the phi-quantum wave-function must undertake to fulfil all its requirements of a-priori definition as the golden-ratio time algorithm, forming an ultimate feedback loop, paying closer attention to the cosmological features at the "end-zone", and how this gives rise to a universal "quantum entanglement" feature that would echo through the entire time-space scheme, as much as the atomic level was scaled up via a process of fractal gauge invariance.

These models represent the universal reference of the “golden ratio” code of time. Other references for  $t_N$  as a general golden ratio algorithm platform for time (and associated process of time seeking to perfect a circle) nonetheless **could** exist beyond the spatial scope of this solar system model (and associated dynamic for time) and thus represent other solar system references, cleaving to the structure of the known perceived universe, leading though nonetheless also to potentially an infinite scope of stellar phenomena of varying stages of temporal development (from golden ratio time growth to collapse) and thus appearance, in theory. In other words, other solar system realities are not being disputed, only that the one that predominates with the golden ratio algorithm of time according to our local reference as humans would appear to be the underlying code of how we would perceive our local reality, despite those other realities beyond this local universal reality of ours potentially representing a different  $t_N$  golden ratio system location and stage of development, a concept which will be addressed more thoroughly in the next paper; in papers 5 [5] and 6 [6] suggestions were made of the stars being an atomic process of outer solar system atomic decay, yet this is resolved as a process by considering the appearance each star as both fitting an independent  $t_N$  reference while still being able to exist “as” that appearance in another  $t_N$  solar system golden ratio reference that fits that appearance, a feature which by its complicated nature needs the scope of a new and subsequent paper to more carefully determine.

It could be argued that if the golden ratio features so well in the process of time, why isn't there *obvious evidence* for it in physics and not just nature? The issue with the golden ratio as an algorithm is that it, the golden ratio for time, is an “*embedded*” algorithm. In fact, it would, as a process of the here and now, time as  $t_N$ , be almost “imperceptible”. Only in cases where the conditions are right and present overlapping/resonant features of time from time-before to time-after “as” those growth patterns of time cast in space, as a footprint, would a golden ratio progression/growth-pattern in time be appreciated. Further to this, the nature of time using the golden ratio presents the case of time as a “singularity”,  $t_N$ , around which we have  $t_B$  and  $t_A$  interplaying in the manner prescribed, namely  $t_A = t_B^2$ , forward (time before to time-after) as the general process of “time” in reality, and backward (time-after to time-before) as the concept of consciousness; features of the golden ratio are embedded in that process, not apparent whatsoever unless viewed as a “complete” structure, whether atomic substructure or universal superstructure, or perhaps in rare cases as a feature of geometrical progression and/or resonance (as seen in crustaceans with their golden ratio stepped-geometrical growth progression). Time indeed surely is one of the great mysteries in physics if an algorithm such as the golden ratio can so efficiently put a vast jigsaw of physical scientific data together using nothing but time.

## Conflicts of Interest

The author declares no conflicts of interest; this has been an entirely self-funded independent project.

## REFERENCES.

1. Jarvis S. H. (2017), Gravity's Emergence from Electrodynamics, <http://vixra.org/abs/1704.0169>, [http://www.equusspace.com/index\\_2.htm](http://www.equusspace.com/index_2.htm)
2. Jarvis S. H. (2017), Golden Ratio Axioms of Time and Space, <http://vixra.org/abs/1706.0488>, [http://www.equusspace.com/index\\_2.htm](http://www.equusspace.com/index_2.htm)
3. Jarvis S. H. (2017), The Emergence of Consciousness from Chaos, <http://vixra.org/abs/1707.0044>, [http://www.equusspace.com/index\\_2.htm](http://www.equusspace.com/index_2.htm)
4. Jarvis S. H. (2017), Phi-Quantum Wave-Function Crystal Dynamics, <http://vixra.org/abs/1707.0352>, [http://www.equusspace.com/index\\_2.htm](http://www.equusspace.com/index_2.htm)

5. Jarvis S. H. (2017), Time as Energy, <http://viXra.org/abs/1711.0419>, [http://www.equusspace.com/index\\_2.htm](http://www.equusspace.com/index_2.htm)
6. Jarvis S. H. (2018), The Relativity of Time, <http://viXra.org/abs/1801.0083>, [http://www.equusspace.com/index\\_2.htm](http://www.equusspace.com/index_2.htm)
7. "Gravitational Potential Energy". hyperphysics.phy-astr.gsu.edu. Retrieved 23 April 2019..
8. Richard Feynman (1970). The Feynman Lectures on Physics Vol I. Addison Wesley. ISBN 978-0 -201-02115-8.
9. "A Universe from Nothing". Astronomical Society of the Pacific. Retrieved 23 April 2019. by Alexei V. Filippenko and Jay M. Pasachoff
10. Alan Guth The Inflationary Universe: The Quest for a New Theory of Cosmic Origins (1997), Random House, ISBN 0-224-04448-6 Appendix A: Gravitational Energy demonstrates the negativity of gravitational energy.
11. Dirac, P.A.M. (1982) [1958]. Principles of Quantum Mechanics. International Series of Monographs on Physics (4th ed.). Oxford University Press. p. 255. ISBN 978-0-19-852011-5.
12. Anderson, C. D. (1933). "The Positive Electron". Physical Review. **43** (6): 491–494. Bibcode:1933PhRv...43..491A. doi:10.1103/PhysRev.43.491
13. Tsan, U. C. (2012). "Negative Numbers And Antimatter Particles". International Journal of Modern Physics E. **21** (1): 1250005. Bibcode:2012IJMPE..2150005T. doi:10.1142/S021830131250005X. Antimatter particles are characterized by negative baryonic number A or/and negative leptonic number L. Materialization and annihilation obey conservation of A and L (associated to all known interactions).
14. Equus Space, <https://www.youtube.com/watch?v=KbQxy8klS-8>, Retrieved 23 April 2019 via YouTube.
15. "The Impossible Propulsion Drive Is Heading to Space". popularmechanics.com. 2 September 2016. Retrieved 23 April 2019.
16. Crew, Bec. "The 'Impossible' EM Drive Is About to Be Tested in Space". sciencealert.com. Retrieved 23 April 2019.
17. "NASA Team Claims 'Impossible' Space Engine Works—Get the Facts". nationalgeographic.com. 21 November 2016. Retrieved 23 April 2019.
18. Seeker (19 November 2016). "How The 'Impossible Drive' Could Break Newton's Third Law". Retrieved 12 July 2018 – via YouTube.
19. Ratner, Paul. "EM Drive, the Impossible Rocket Engine, May Be Closer to Reality". bigthink.com. Retrieved 23 April 2019.
20. Poitras, Colin (December 7, 2016). "To Mars in 70 days: Expert discusses NASA's study of paradoxical EM propulsion drive". Phys.org. Retrieved 23 April 2019.
21. Drake, Nadia; Greshko, Michael (21 November 2016). "NASA Team Claims 'Impossible' Space Engine Works—Get the Facts". Nationalgeographic.com: National Geographic. Retrieved 23 April 2019.
22. <https://arstechnica.com/science/2018/05/nasas-em-drive-is-a-magnetic-wtf-thruster/>. Retrieved 23 April 2019.
23. <https://news.nationalgeographic.com/2018/05/nasa-emdrive-impossible-physics-independent-tests-magnetic-space-science/>. Retrieved 23 April 2019.